EZH2-mediated suppression of lncRNA-LET promotes cell apoptosis and inhibits the proliferation of post-burn skin fibroblasts

WEICAI ZHENG and AIXIANG YU

Department of Burns and Plastic Surgery, The First Affiliated Hospital of Henan University of Science and Technology, College of Clinical Medicine of Henan University of Science and Technology, Luoyang, Henan 471003, P.R. China

Received September 14, 2016; Accepted November 9, 2017

DOI: 10.3892/ijmm.2018.3425

Abstract. Although the upregulation of enhancer of zeste homolog 2 (EZH2) expression and downregulation of long non-coding RNA (lncRNA) LET expression are known to be associated with cell apoptosis and proliferation, little is known about the interaction of EZH2 with lncRNA LET. The present study aimed to investigate the interaction of EZH2 and lncRNA LET, and the mechanism of human dermal fibroblast (HDF) proliferation and apoptosis. Tissue samples from 33 burn patients with second- and third-degree burns and 8 controls were collected. mRNA was extracted from the burn tissues for analysis. Isolated primary HDFs were treated with heat or transfected with LET overexpression vectors, and the cell functions and associated proteins in the HDFs were analyzed. Decreased lncRNA LET expression was detected in burn tissues compared with normal skin. Heat-treated HDFs exhibited a reduction in lncRNA LET expression and increase in EZH2 expression. LET gain-of-function experiments in primary HDFs revealed increases in cell proliferation, the proportion of cells in the S stage, and cyclin D1 and cyclin-dependent kinase 4 (CDK4) expression, and reductions in the percentage of apoptotic cells, the Bax/Bcl-2 ratio and caspase-3 expression. RNA immunoprecipitation and chromatin immunoprecipitation assays demonstrated the interaction of ZH2 with lncRNA LET, and of EZH2 with H3K27me3 in HDFs. Furthermore, a negative correlation between lncRNA LET and EZH2 expression was identified. It may be concluded that increased lncRNA-LET expression promoted cell proliferation and inhibited cell apoptosis via the cyclin D1-CDK4 and Bax/Bcl-2/caspase-3 signaling pathways, respectively. Furthermore, the inhibition of lncRNA LET may be regarded as an option for use in the healing of burns.

Correspondence to: Professor Weicai Zheng, Department of Burns and Plastic Surgery, The First Affiliated Hospital of Henan University of Science and Technology, College of Clinical Medicine of Henan University of Science and Technology, 24 Jinghua Road, Jianxi, Luoyang, Henan 471003, P.R. China
E-mail: weicaizheng28@126.com

Key words: long non-coding RNA LET, burn, cell proliferation, enhancer of zeste homolog 2, skin fibroblast

Introduction

Burn injury disrupts the protective skin barrier by inducing various reactions, including increased metabolism, moisture loss and immune system malfunction, with the majority of severely burned patients exhibiting dysfunction of the immune system (1,2). The proliferation of keratinocytes, vascular endothelial cells and dermal fibroblasts serves an important role in wound healing (3,4). In addition, the proliferation and growth of these cells is regulated by numerous factors associated with immune system malfunction, cell proliferation and cell apoptosis.

Long non-coding RNAs (lncRNAs) have been demonstrated be essential for the immune response, cell proliferation and the apoptosis of dermal fibroblasts (5-7). Zhu *et al* (7) demonstrated that the expression of lncRNA-activated by transforming growth factor (TGF)-β and its target zinc finger protein 217 in keloid fibroblasts promoted the autocrine secretion of TGF-β2, and thereby promoted scar formation. In addition, the detection of the lncRNA CACNA1G-AS1 in keloids indicated that lncRNAs are crucial for keloid formation (8).

The lncRNA low expression in tumor (LET), a recently identified lncRNA, is suppressed by enhancer of zeste homolog 2 (EZH2) (5). EZH2, the catalytic subunit of polycomb repressive complex 2 (PRC2), is responsible for epigenetic silencing through histone H3 lysine 27 trimethylation (H3K27me3) (9). EZH2 and H3K27me3 are expressed in several human tumors and are positively associated with high cancer cell proliferation rates and poor clinical outcomes (9-11), suggesting that EZH2-mediated H3K27me3 has oncogenic activity (10,12). Furthermore, the effect of EZH2 on cell proliferation has been demonstrated in numerous studies, in which the downregulation or suppression of EZH2 expression was essential for the enhancement of cell apoptosis (13-16). In addition, the expression of EZH2 and H3K27me3 has been detected in inflammatory disorders, including rheumatoid arthritis (17) and colitis (18). Although the elevated expression of EZH2 and downregulation of lncRNA LET have been detected in invasive cancer tissues and cancer cells, apoptosis and disease pathogenesis (19-21),

studies focusing on the interaction of EZH2 and lncRNA LET in the modulation of cell proliferation and apoptosis are lacking.

The present study aimed to investigate the interaction of EZH2 and lncRNA LET, and the mechanism underlying its effect on in human dermal fibroblast (HDF) proliferation and apoptosis. Tissue samples were collected from burn patients for analysis. Isolated primary HDFs were transfected with LET overexpression vectors to explore the effect of LET on cell proliferation and cell apoptosis. The interactions of LET with EZH2, and of EZH2 with H3K27me3 were determined in order to elucidate the roles of lncRNA LET, EZH2 H3K27me3, and cell cycle- and apoptosis-related proteins in the regulatory mechanism of HDFs. This study may for the first time, to the best of our knowledge, provide information on the interaction of EZH2 and lncRNA LET in the modulation of cell proliferation and apoptosis, and its potential application to burn wound-healing therapy.

Materials and methods

Tissue sample collection. A total of 33 samples were collected from 21 male and 12 female patients (mean age, 31.4 years) at the Department of Burns and Plastic Surgery of the First Affiliated Hospital of Henan University of Science and Technology (Luoyang, China) between January 10, 2014 and February 20, 2015. Patients with any of the following exclusion criteria were not included in the present study: Children under the age of 12 years, individuals older than 80 years, severe complications of burns, diagnosis with or history of diabetes, long-term hormone intake, malignant tumors, and receipt of chemoradiotherapy. All burns documented in this study were second- and third-degree burns from patients admitted <24 h after the time of burn injury (22). Patients were then classified into three classes of burn injury: Slight (n=16), moderate (n=20) and severe (n=7), according to the severity of the burn injury (23). Eight normal control skin tissues were collected from healthy volunteers who had undergone plastic surgery procedures at the same department and hospital. Informed consent from the 43 patients and approval from the Ethics Committee of the College of Clinical Medicine of Henan University were obtained prior to the study.

Primary HDF culture. Primary HDFs were derived from normal human skin collected from patients who had undergone plastic surgery procedures in the Department of Burns and Plastic Surgery, as previously described (24). Informed consent was obtained from the participants and approval was provided by the Ethics Committee of the College of Clinical Medicine of Henan University. In brief, the normal skin tissues were dissected and cut into small pieces, washed with phosphate-buffered saline, and then digested with 0.05% trypsin-EDTA solution (Sigma-Aldrich; Merck KGaA, Darmstadt, Germany) for 30 min. Subsequently, isolated cells were cultured in standard culture conditions comprising Dulbecco's modified Eagle's medium (DMEM; Thermo Fisher Scientific, Inc., Waltham, MA, USA) combined with penicillin-streptomycin (100 U; Invitrogen; Thermo Fisher Scientific, Inc.) and 10% fetal bovine serum (FBS; Sigma-Aldrich; Merck KGaA) at 37˚C with 5% CO_2. In addition, cell cultures were placed into a water heater tank and incubated at 52˚C for 30 sec to obtain heat-treated HDFs. The HDFs were maintained under the standard culture conditions and used at passages 5-8 throughout the experiments in the present study. 293 cells (CRL-1573; ATCC, Manassas, VA, USA) were cultured in DMEM (10% FBS, penicillin-streptomycin) at 37˚C with 5% CO_2.

Cell transfection. To observe the effects of lncRNA-LET overexpression on HDF functions, an lncRNA-LET overexpression plasmid vector (pc-LET; 50 nM) was constructed using cDNA with a functional region. Pc-EZH2 and short interfering RNA (siRNA)-EZH2 plasmids (50 nM) were constructed for cell transfection. Plasmids were transfected into HDFs using Lipofectamine® 2000 (Thermo Fisher Scientific, Inc.). Cells (density, $2x10^5$) were then cultured for 24-48 h for use in the experiments. Cells without any vector transfection were used as control. The primer for silenced LET (si-LET) is as follows: 5'-TGGGAGTAAAGGGAAAGAGTT-3'.

Cell viability assay. Primary HDFs were seeded at a density of $1x10^4$ cells/well into 96-well plates and incubated for 24-48 h for cell transfection. The viability of the transfected and untransfected cells was determined using an MTT assay at 0, 12, 24 and 48 h after transfection (25). The optical density at 540 nm was detected and used to plot a proliferation curve.

Clonogenic assay. A clonogenic assay of the primary HDFs was performed using a method based on that described by Jiao *et al* (26). Cells were maintained in DMEM, transfected with pc-LET, seeded in 6-well plates at a final density of 1,000 cells/well, and cultured for 14 days at 37˚C. The HDFs were then fixed with 4% paraformaldehyde at room temperatire for 2 h, stained with Diff-Quick (Diff-Quick, Protocol HEMA 3 stain; Thermo Fisher Scientific, Inc.,), and air dried. Colonies with ≥30 cells were counted using a microscope (IX83; Olympus Corporation, Tokyo, Japan). All experiments were performed in triplicate.

Cell cycle evaluation. Trypsin-digested primary HDFs were seeded into 6-well plates at a density of $5x10^4$ cells/well and incubated for 24 h. The HDFs were then harvested, centrifuged and fixed with ethanol at 4˚C for 24 h. The fixed HDFs were treated with propidium iodide (PI; Clontech Laboratories, Inc., Mountain View, CA, USA). Finally, the cell cycle was analyzed using a FACSCanto flow cytometer and CellQuest software version 5.1 (both BD Biosciences, San Jose, CA, USA). All detections were performed in three triplicates. The proportion of proliferative cells was calculated as follows: Proliferative proportion = (S + G1/M) cells / total cells stained with PI.

Cell apoptosis assay. HDFs (density, $1x10^5$) seeded on 24-well plates were maintained for 24 h. The cell cultures were supplemented with Annexin V-fluorescein isothiocyanate (FITC) and PI (Clontech Laboratories, Inc.) for 10 min in the dark. Finally, the FACSCanto flow cytometer was used to analyze cell apoptosis. Annexin V-positive and PI-negative cells were considered to be apoptotic cells.

RNA isolation and reverse transcription-quantitative polymerase chain reaction (RT-qPCR). Total RNA from the burn tissues and HDF cells was extracted using TRIzol reagent (Invitrogen; Thermo Fisher Scientific, Inc.) and purified with RNase-free Dnase I (Promega Corporation, Madison, WI,

Table I. Primer sequences.

Gene name	Primer sequences (5'-3')
LET	F: 5'-GGAGTAAAGGGAAAGAGTTGC-3'
	R: 5'-GTGTCGTGGACTGGCAAAAT-3'
EZH2	F: 5'-CAGCCTTGTGACAGTTCGT-3'
	R: 5'-AGATGGTGCCAGCAATAGA-3'
Bax	F: 5'-TGCCCGAAACTTCTAAAA-3'
	R: 5'-CGTGACTGTCCAATGAGC-3'
Bcl-2	F: 5'-GCAGAAGTCTGGGAATCG-3'
	R: 5'-GCATAAGGCAACGATCC-3'
Caspase-3	F: 5'-ACCGATGTCGATGCAGCTAA-3'
	R: 5'-AGGTCCGTTCGTTCCAAAAA-3'
Cyclin D1	F: 5'-GCTGCTCCTGGTGAACAAGC-3'
	R: 5'-CACAGAGGGCAACGAAGGTC-3'
CDK4	F: 5'-TGCCAATTGCATCGTTCACCGAG-3'
	R: 5'-TGCCCA ACTGGTCGGCTTCA-3'
Cyclin A1	F: 5'-CGCACAGAGACCCTGTACTT-3'
	R: 5'-TTGGAACGGTCAGATCAAAT-3'
Cyclin E1	F: 5'-GTTATAAGGGAGACGGGGAG-3'
	R: 5'-TGCTCTGCTTCTTACCGCTC-3'
GAPDH	F: 5'-GGAGCGAGATCCCTCCAAAAT-3'
	R: 5'-GGCTGTTGTCATACTTCTCATGG-3'

LET, low expression in tumor; EZH2, enhancer of zeste homolog 2; Bax, Bcl-2-associated X protein; Bcl-2, B-cell lymphoma 2; CDK, cyclin-dependent kinase 4; F, forward; R, reverse.

USA). The purified RNA was then used for cDNA synthesis. The expression of certain genes in the burn tissues or HDF cells was detected using a SYBR ExScript qRT-PCR kit (Takara Biotechnology Co., Ltd, Dalian, China) on an ABI 7500 system (Applied Biosystems; Thermo Fisher Scientific, Inc.). Primer sequences are listed in Table I. The LET primers were synthesized by Shanghai Sangon Biological Engineering Technology and Services Co., Ltd. (Shanghai, China). A final 20-μl reaction mixture was amplified using the following reaction conditions: Initial desaturation at 95˚C for 5 min, followed by denaturation at 95˚C for 30 sec, annealing at 60˚C for 40 sec and extension at 72˚C for 10 sec for 40 cycles. GAPDH was used as an internal control for mRNA or lncRNAs. All reactions were run in triplicate. PCR products were resolved on 2% agarose, visualized with ethidium bromide staining, and analyzed using a FluorChem 8900 imager (ProteinSimple, San Jose, CA, USA). The relative mRNA expression level was calculated by the $2^{-\Delta\Delta Cq}$ method (27).

Semi-quantitative RT-PCR. The expression of si-EZH2 and IgG were analyzed using semi-quantitative RT-PCR. Total RNA was extracted with TRIzol reagent (Invitrogen; Thermo Fisher Scientific, Inc.), and RT-PCR was performed with a PCR kit from Fermentas (Hanover, MD, USA). The primers used for amplification were shown in Table I. The PCR profile was listed as follows: 94˚C for 2 min followed by 35 cycles of 94˚C for 30 sec, 58˚C for 30 sec, and 72˚C for 30 sec, with a final extension at 72˚C for 10 min.

Western blot assay. Transfected primary HDFs were seeded into 6-well plates at a density of $1.0x10^6$ in DMEM and harvested at 48 h after transfection. Cells were then lysed using radioimmunoprecipitation assay buffer (Beijing Solarbio Bioscience and Technology Co., Ltd., Beijing, China) and protein was quantified using a BCA protein assay kit (Thermo Fisher Scientific, Inc.). Equal amounts of protein (20 μg) were separated using 10% SDS-PAGE gels and transferred onto polyvinylidene difluoride (PVDF) membranes (Invitrogen; Thermo Fisher Scientific, Inc.). The PVDF membranes were then blocked with 5% skimmed milk (BD Biosciences) and incubated with primary antibody against cyclin D1 (dilution 1:1,000; ab134175), cyclin-dependent kinase 4 (CDK4; dilution 1:1,000; ab199728), cyclin E1 (dilution 1:1,000; ab33911), cyclin A1 (dilution 1:1,000; ab118897), B-cell lymphoma 2 (Bcl-2; dilution 1:1,000; ab59348), Bcl-2-associated X protein (Bax; dilution 1:2,000; ab53154), cleaved caspase-3 (dilution 1:1,000; ab32042), EZH2 (dilution 1:500; ab186006) and GAPDH (dilution 1:2,000; ab181602) at 4˚C overnight. The membranes were then incubated with horseradish peroxidase-conjugated secondary antibodies (1:1,000 dilution; ab9482) for 1 h at room temperature. All antibodies were purchased from Abcam (Cambridge, UK). The bands of the target proteins were visualized and analyzed with Enhanced Chemiluminescence (ECL) reagent (GE Healthcare Life Sciences) using the Tanon-5200 Chemiluminescent Imaging system (Tanon Science and Technology Co., Ltd., Shanghai, China).

Chromatin immunoprecipitation (ChIP) assay. As described by Luo *et al* (16), a ChIP assay was performed using an EZ-ChIP™ Chromatin Immunoprecipitation kit (EMD Millipore, Billerica, MA, USA). Firstly, cross-linked chromatin was sonicated into fragments in the size range 200-1,000 bp, and the fragments were immunoprecipitated using H3K27me3 antibody (dilution 1:500; SAB4800015; Sigma-Aldrich; Merck KGaA). Normal human immunoglobulin G (IgG; dilution 1:500; ab7461; Abcam) was chosen as the negative control. Semi-quantitative RT-PCR was conducted as described above.

RNA immunoprecipitation (RIP) assay. An RIP assay was performed using a Magna RIP™ RNA-Binding Protein Immunoprecipitation kit (EMD Millipore) as described by Luo *et al* (16). Anti-EZH2 antibody and IgG (control) were used for RIP [anti-EZH2 (dilution 1:1,000; 4905), anti-IgG (dilution 1:1,000; 147008); Cell Signaling Technology, Inc., Danvers, MA, USA]. Coprecipitated RNAs were purified and cDNA was synthesized for analysis by RT-qPCR. Total RNAs (input controls) and isotype controls were detected simultaneously to demonstrate that the detected signals were the results of RNAs specifically binding to EZH2.

Statistical analysis. All data are expressed as mean ± standard deviation from three triplicates. Data were analyzed using Graph Prism 6.0 software (GraphPad Prism, Inc., La Jolla,

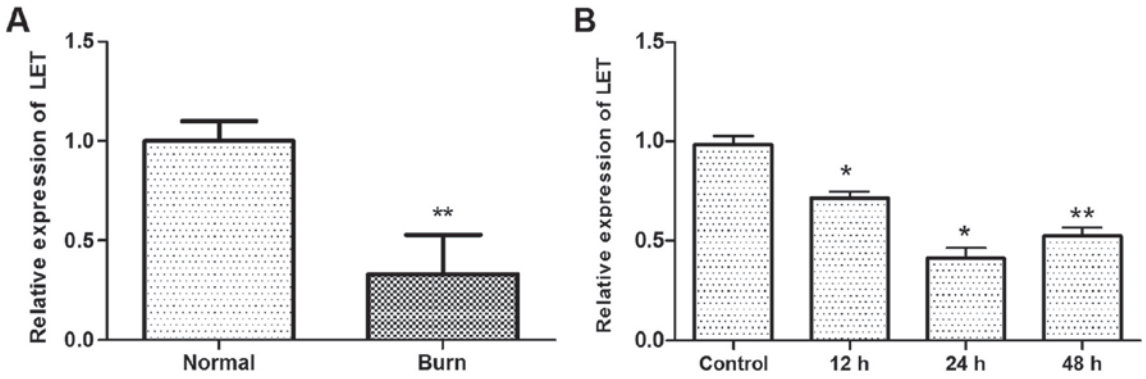

Figure 1. Expression of (A) long noncoding LET in burn injury and normal skin tissues and (B) human primary HDFs. The HDFs were exposed to 52˚C heat in a water heater and evaluated at 12, 24 and 48 h following heat damage. *P<0.05 and **P<0.01 vs. normal or control, respectively. HDF, human dermal fibroblast; LET, low expression in tumor.

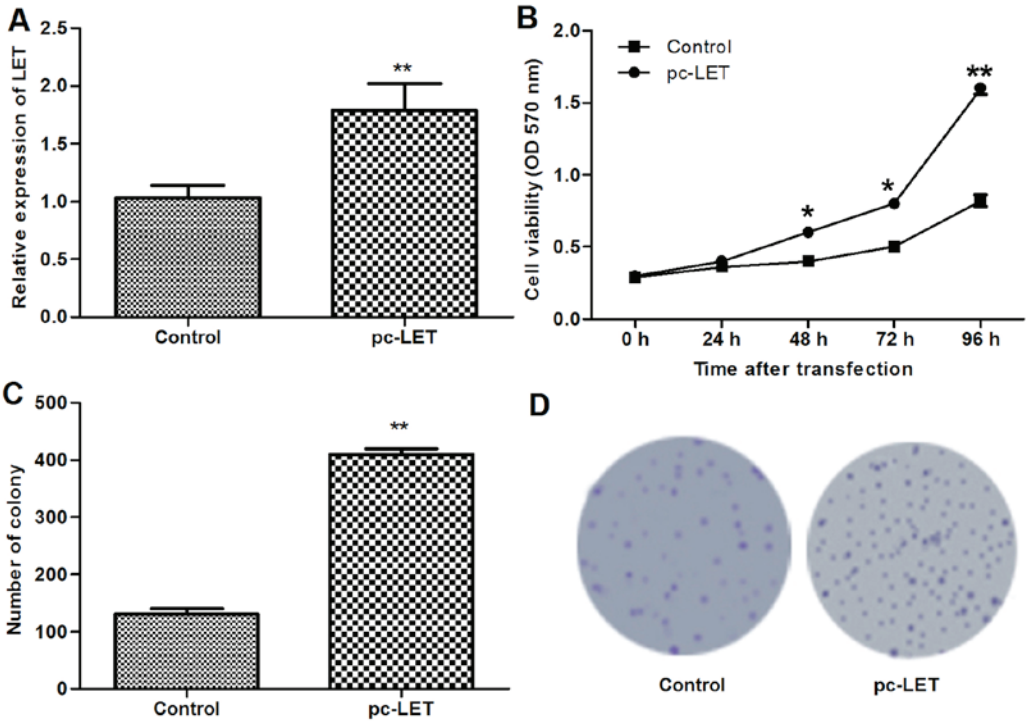

Figure 2. LET overexpression promotes HDF proliferation. Primary HDFs were transfected with pc-LET overexpression plasmid. (A) LET mRNA expression was evaluated by reverse transcription-quantitative polymerase chain reaction. Cell viability and cell colony formation were assessed using (B) MTT and (C) clonogenic assay. In the clonogenic assay, (D) cell colonies were stained with Diff-Quick (magnification x400). *P<0.05 and **P<0.01 vs. control. HDF, human dermal fibroblast; LET, low expression in tumor; OD, optical density.

CA, USA). Student's t-test and Tukey's test were used to analyze differences between and among groups, respectively. Correlation between lncRNA LET and EZH2 was analyzed using Pearson correlation coefficient. P<0.05 was considered to indicate a statistically significant result.

Results

Heat treatment inhibits the expression of LET. The expression of lncRNA LET was downregulated in tissues from burn injury compared with normal HDFs (P<0.01; Fig. 1A). In addition, the expression of LET was lower in primary HDFs treated with heat compared with the control (P<0.05 at 12 h and 24 h, P<0.01 at 48 h; Fig. 1B). The lowest expression of LET in the HDFs was observed at 24 h following the heat treatment. These results demonstrate that LET expression is inhibited by heat.

LET overexpression promotes cell proliferation. The LET overexpression plasmid pc-LET was constructed and transfected into heat-treated HDFs for 24 h. RT-qPCR analysis demonstrated that LET mRNA was upregulated in the transfected HDFs compared with the untransfected HDFs (P<0.01; Fig. 2A). The MTT assay indicated that the LET overexpression induced in the HDFs following transfection with pc-LET significantly increased cell viability compared with that of untransfected HDFs (P<0.01; Fig. 2B). In addition, the number of colonies formed by the

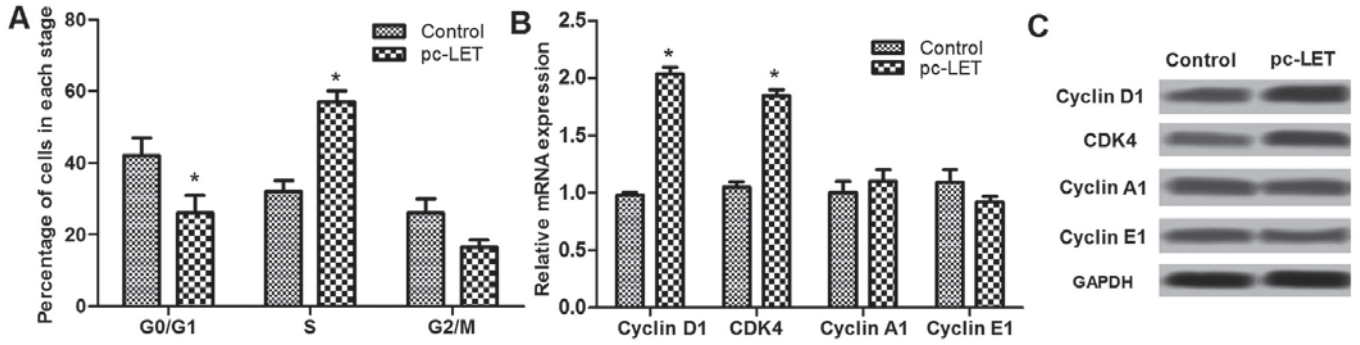

Figure 3. LET overexpression regulates the cell cycle of human dermal fibroblasts via cell cycle-associated proteins. (A) Cell cycle analysis was conducted using flow cytometry. (B) The mRNA expression of cell cycle-associated factors was analyzed using reverse transcription-quantitative polymerase chain reaction and (C) the protein levels were analyzed by western blotting. *P<0.05 vs. control. LET, low expression in tumor; pc-LET, LET overexpression plasmid; CDK4, cyclin-dependent kinase 4.

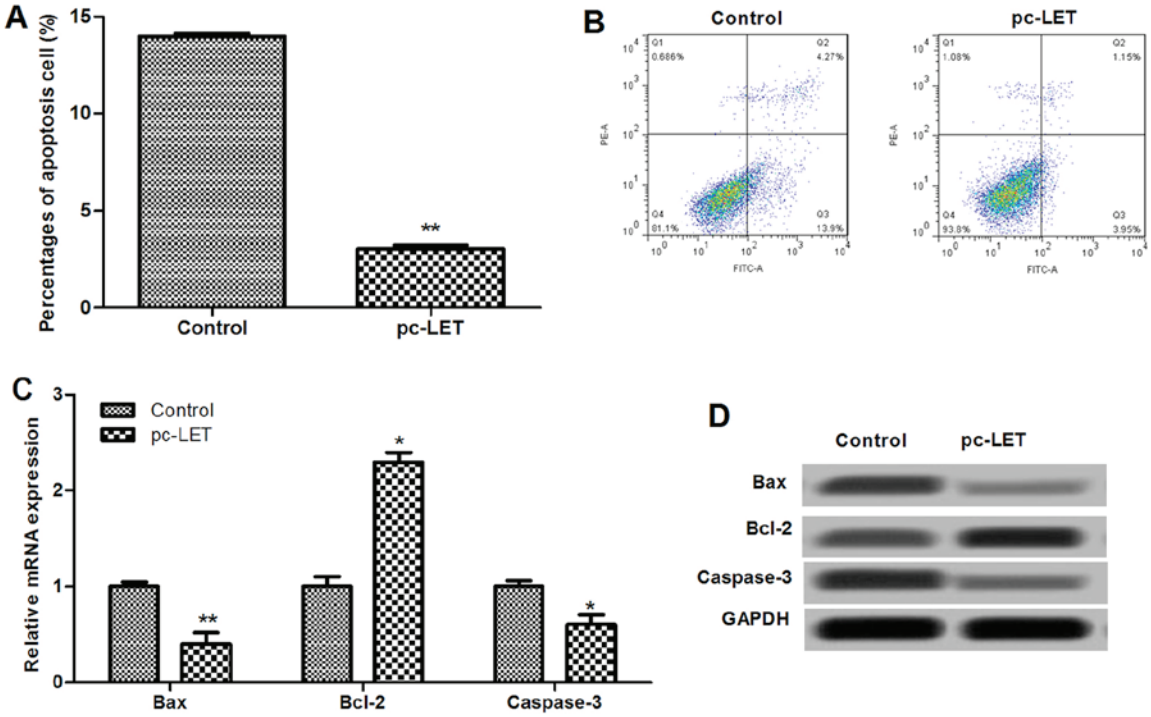

Figure 4. Transfection with pc-LET inhibits the apoptosis of human dermal fibroblasts. (A) The percentage of apoptotic cells was determined by (B) flow cytometry using Annexin V-fluorescein and propidium iodide dual staining. (C) The mRNA expression of apoptosis-associated factors was analyzed by reverse transcription-quantitative polymerase chain reaction and (D) the protein levels were analyzed by western blotting. *P<0.05 and **P<0.01 vs. control. LET, low expression in tumor; pc-LET, LET overexpression plasmid; Bax, Bcl-2-associated X protein; Bcl-2, B-cell lymphoma 2.

transfected HDFs was significantly increased compared with the control (P<0.01; Fig. 2C and D). These results demonstrate that pc-LET increased the proliferation of the HDFs.

LET overexpression regulates the cell cycle at the G1 stage. Analysis of the cell cycle using flow cytometry revealed that pc-LET transfection significantly reduced the percentage of cells in the G0/G1 stage, and upregulated the percentage of cells in the S stage (P<0.05; Fig. 3A). Analysis of cell cycle-related factors, including cyclin D1, CDK4, cyclin A1 and cyclin E1 by RT-qPCR demonstrated that the expression of some of these factors was dysregulated by pc-LET transfection. Cyclin D1 and CDK4 mRNA levels were significantly increased by pc-LET transfection, compared with those in the control HDFs (P<0.05; Fig. 3B). However, cyclin A1 and cyclin E1 expression were not markedly regulated by pc-LET transfection. In addition, the dysregulated expression levels of cyclin D1, CDK4, cyclin A1 and E1 were shown in Fig. 3C. These results show that LET promotes HDF proliferation via cell cycle arrest at the S stage through the upregulation of cyclin D1 and CDK4.

LET overexpression inhibits cell apoptosis. Flow cytometry with Annexin V-FITC and PI dual staining indicated that LET overexpression significantly inhibited the apoptosis of HDFs (P<0.01; Fig. 4A and B). Results showed that the

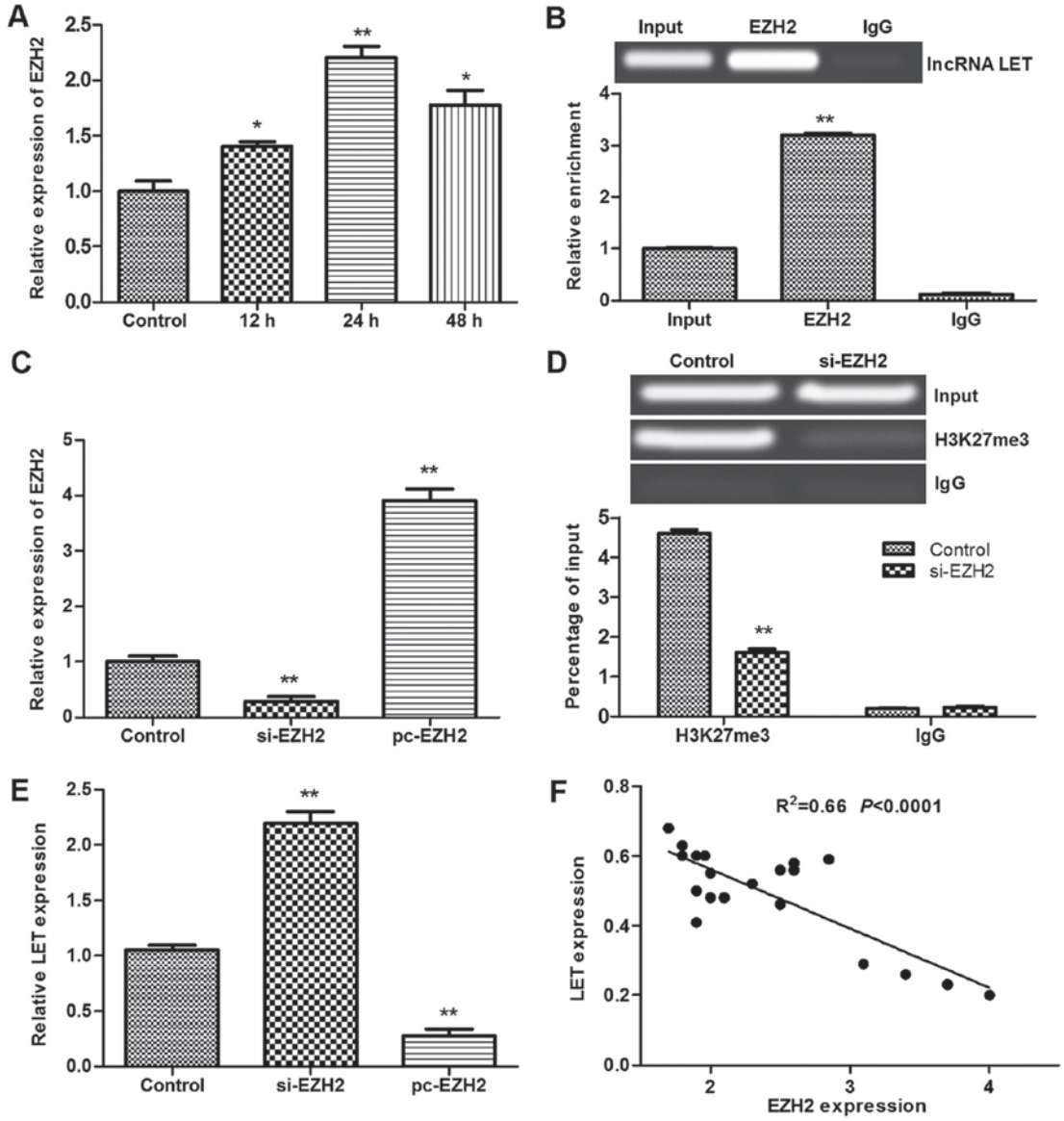

Figure 5. Results of RIP and ChIP assays for primary HDFs. (A) Relative expression of EZH2 in heat-treated HDFs. (B) RIP analysis was performed using antibodies against EZH2 and IgG. (C) pc-EZH2 and si-EZH2 were transfected into HDFs. (D) ChIP analysis was performed using antibodies against H3K27me3 and IgG. (E) Relative expression of LET in HDFs transfected with pc-EZH2 or si-EZH2. (F) Correlation of LET and EZH2 expression in burn tissues from patients. *P<0.05 and **P<0.01 vs. control or input, respectively. RIP, RNA immunoprecipitation; ChIP, chromatin immunoprecipitation; HDF, human dermal fibroblast; EZH2, enhancer of zeste homolog 2; IgG, immunoglobulin G; pc-EZH2, EZH2 overexpression plasmid; si-EZH2, EZH2, small interfering RNA; LET, low expression in tumor; lncRNA, long non-coding RNA; H3K27me3, histone H3 lysine 27 trimethylation.

mRNA expression of cell apoptosis-associated proteins, including Bax, Bcl-2 and cleaved caspase-3, were dysregulated by pc-LET transfection compared with those in the control (P<0.05; Fig. 4C). The protein levels of the cell apoptosis-related proteins were also analyzed using western blotting (Fig. 4D). The expression levels of Bax and cleaved caspase-3 in the pc-LET transfected HDFs were significantly lower than those in the control (P<0.05). However, the expression of Bcl-2 was upregulated in the pc-LET transfected HDFs compared with the control (P<0.05). These results indicate that pc-LET transfection inhibits cell apoptosis through downregulation of the Bax/Bcl-2 ratio and caspase-3.

Association of LET with EZH2 is involved in cell growth and apoptosis. lncRNAs have been shown to serve crucial roles in the proliferation of skin fibroblasts (28). EZH2 is indicated to be a transcription factor of H3K27me3, and a combination of these two factors is essential for the pathogenesis and development of various diseases (28,29). To investigate the association of EZH2 and H3K27me3 with LET in primary HDFs derived from burned skin, RIP and ChIP analyses were conducted. The results demonstrated that EZH2 was upregulated in heat-treated HDF cells at 12-48 h after heat exposure (Fig. 5A). The expression of EZH2 mRNA was significantly upregulated by heat treatment, and the highest expression was observed at 24 h post-treatment (P<0.01 vs. control). The RIP analysis revealed that EZH2 was enriched in the HDFs by binding to LET (Fig. 5B). Furthermore, following transfection with siRNA-EZH2 (Fig. 5C), ChIP analysis revealed an interaction between H3K27me3 and EZH2 (Fig. 5D). Analysis of LET and

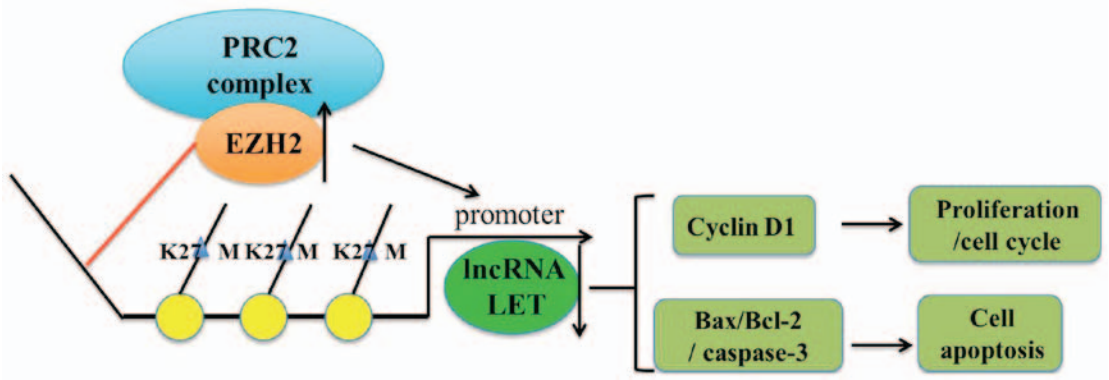

Figure 6. Model for the H3K27me3 dependent EZH2-LET interaction mechanism. Both H3K27me3 and EZH2-LET interaction were essential for expression of lncRNA LET, and the downstream proteins related to cell proliferation and apoptosis. Three methylation sites of EZH2 at H3K27me3 promoter are presented by three yellow balls. EZH2-catalyzed H3K27me3 trimethylation inhibits lncRNA-LET expression and promotes cell apoptosis. H3K27me3, histone H3 lysine 27 trimethylation; EZH2, enhancer of zeste homolog 2; LET, low expression in tumor; lncRNA, long non-coding RNA; PRC2, polycomb repressive complex 2; Bax, Bcl-2-associated X protein; Bcl-2, B-cell lymphoma 2.

EZH2 expression in the HDFs (Fig. 5E) and burn tissues from patients (Fig. 5F) revealed that there was a negative correlation between LET and EZH2 expression. These results suggest that the elevated expression of EZH2 in burned HDFs inhibits LET by binding to it, thus suppressing H3K27me3 expression and modulating cell proliferation and apoptosis (Fig. 6).

Discussion

Previous studies have shown that the interaction of lncRNA with EZH2 is associated with cancer cell metastasis (16,30), proliferation (14,31) and apoptosis (13,14) by target modulation, implicating the role of EZH2 and lncRNA in cell proliferation. The present study aimed to investigate the interaction of EZH2 and lncRNA LET, and its involvement in the mechanism of HDF proliferation and apoptosis. The results demonstrated that there was a negative correlation between EZH2 and lncRNA LET expression in burned skin tissues and HDFs subjected to heat treatment. Transfection with pc-LET promoted HDF proliferation, arrested the cell cycle at the S stage, and inhibited cell apoptosis via modulation of the cell cycle and apoptosis-associated proteins.

EZH2, the catalytic subunit of PRC2, is a core epigenetic regulator that has a crucial role in cell proliferation, cell fate decisions, cancer initiation and the response of cells to inflammation (9,32). EZH2 and H3K27me3 expression has been observed to be positively associated with high cancer cell proliferation rates and poor clinical outcomes (9-11), which indicates that the EZH2-mediation of H3K27me3 is oncogenic (10,12). In addition, the high expression of EZH2 and H3K27me3 has been detected in synovial fibroblasts in rheumatoid arthritis and fibroblasts associated with renal fibrogenesis (17), in accordance with studies indicating that EZH2-mediated H3K27me3 increase is involved in the inflammatory response (32-34). DuPage *et al* demonstrated a critical role for EZH2 in the maintenance of regulatory T (Treg) cell identity during cellular activation, with EZH2-deficient Treg cells being destabilized and lacking the ability to prevent autoimmunity (32). In the present study, the expression of EZH2 in primary HDFs was increased following heat treatment compared with that in the control. Furthermore, the positive association of H3K27me3 expression with EZH2 was revealed by ChIP analysis. These results indicate that the upregulation of EZH2 and EZH2-mediated H3K27me3 serve major roles in the fate decision of HDF cells from burned skin, which may benefit autoimmunity and the cell response to inflammation.

In the present study, analysis of the association between lncRNA LET downregulation and EZH2 overexpression in burned human skin tissues revealed a negative correlation. In addition, in lncRNA-LET gain-of-function experiments in which pc-LET overexpression plasmids were transfected into HDFs, increased cell viability and clone formation, and a reduced proportion of apoptotic cells were observed. These results reveal that the expression of lncRNA LET in primary HDF cells promoted cell proliferation and inhibited cell apoptosis. This was in accordance with the negative association of lncRNA LET and EZH2 expression in hepatocellular carcinoma observed by Sun *et al* (5). Sun *et al* (5) reported that the loss of expression of lncRNA-LET in nasopharyngeal carcinoma (NPC) tissues was negatively associated with risk factors and clinical features including advanced clinical stage and poor patient survival, and EZH2 expression. Furthermore, lncRNA-LET gain- and loss-of-function experiments conducted in that study demonstrated that LET overexpression inhibited EZH2 expression and NPC cell proliferation, and promoted NPC cell apoptosis. By contrast, the silencing of LET using siRNA promoted cell proliferation and inhibited cell apoptosis. An association of low lncRNA-LET with poor prognosis was also reported in gastric cancer by Zhou *et al* (21). Together, these results demonstrate that the decreased expression of lncRNA LET is a poor prognosis factor for tumors and burn-injured patients. Furthermore, the upregulation of lncRNA LET may be regarded as a therapeutic intervention option for cancer and burns.

Since lncRNA LET expression contributes to the proliferation and apoptosis of cancer cells and human primary HDFs, the expression of cell cycle- and apoptosis-related proteins in pc-LET transfected cells was investigated in the present study. The cell cycle and apoptosis are complicated processes involving numerous genes and signaling pathways (35-38). Bcl-2, Bax and caspase-3 are important factors for cell apoptosis, and an increase in the Bax/Bcl-2 ratio may promote cell apoptosis (35,36,39,40). Furthermore, cyclin D1 and CDK4/6 are

essential for maintaining cell cycle progression, and inhibition of the cyclin D1-CDK4/6 pathway may arrest the cell cycle with cell accumulation at the G0/G1 stage (41,42). The observation that enhanced lncRNA LET expression significantly upregulated the expression of cyclin D1 and CDK4, altered the progression of cells from the G0/G1 stage to the S stage, and inhibited cyclin E1, an oncogene (43), indicates that lncRNA LET modulates the cell cycle via the cyclin D1-CDK4 signaling pathway.

The observation that increased lncRNA LET expression significantly inhibited cell apoptosis and downregulated the Bax/Bcl-2 ratio and cleaved caspase-3 expression indicate that lncRNA LET inhibits cell apoptosis through the Bax/Bcl-2/caspase-3 signaling pathway. Thus, the present study demonstrates that lncRNA LET inhibits cell apoptosis and promotes cell proliferation via Bax/Bcl-2/caspase-3 and cyclin D1-CDK4 signaling pathways, respectively, in HDFs.

In conclusion, the results of the present study indicate that in burns, the reduced expression of lncRNA LET and upregulation of EZH2 promote cell apoptosis and inhibit the proliferation of HDFs. Furthermore, a negative correlation between lncRNA LET and EZH2 expression was detected in burn-injured tissues. RIP and ChIP analysis confirmed the interaction of EZH2 with lncRNA LET, and EZH2 with H3K27me3. The LET gain-of-function experiment using primary HDFs suggests that increased lncRNA-LET expression promoted cell proliferation and inhibited cell apoptosis via the cyclin D1-CDK4 and Bax/Bcl-2/caspase-3 signaling pathways, respectively. From these observations, it may be speculated that the upregulation of lncRNA LET is a potential therapeutic intervention for burn wound healing. However, the mechanism of action of lncRNA LET in cell apoptosis and proliferation, as well as the direct target proteins of lncRNA LET, require further exploration.

Competing interests

The authors declare that they have no competing interests.

References

1. Patil NK, Bohannon JK, Luan L, Guo Y, Fensterheim B, Hernandez A, Wang J, Sherwood ER: FLT3 ligand treatment attenuates T cell dysfunction and improves survival in a murine model of burn wound sepsis. Shock 47: 40-51, 2017.
2. Xiu F and Jeschke MG: Perturbed mononuclear phagocyte system in severely burned and septic patients. Shock 40: 81-88, 2013.
3. Chigurupati S, Mughal MR, Okun E, Das S, Kumar A, McCaffery M, Seal S and Mattson MP: Effects of cerium oxide nanoparticles on the growth of keratinocytes, fibroblasts and vascular endothelial cells in cutaneous wound healing. Biomaterials 34: 2194-2201, 2013.
4. Nauta A, Seidel C, Deveza L, Montoro D, Grova M, Ko SH, Hyun J, Gurtner GC, Longaker MT and Yang F: Adipose-derived stromal cells overexpressing vascular endothelial growth factor accelerate mouse excisional wound healing. Mol Ther 21: 445-455, 2013.
5. Sun Q, Liu H, Li L, Zhang S, Liu K, Liu Y and Yang C: Long noncoding RNA-LET, which is repressed by EZH2, inhibits cell proliferation and induces apoptosis of nasopharyngeal carcinoma cell. Med Oncol 32: 226, 2015.
6. Wang Z, Jinnin M, Nakamura K, Harada M, Kudo H, Nakayama W, Inoue K, Nakashima T, Honda N, Fukushima S, *et al*: Long non-coding RNA TSIX is upregulated in scleroderma dermal fibroblasts and controls collagen mRNA stabilization. Exp Dermatol 25: 131-136, 2016.
7. Zhu HY, Bai WD, Li C, Zheng Z, Guan H, Liu JQ, Yang XK, Han SC, Gao JX, Wang HT, *et al*: Knockdown of lncRNA-ATB suppresses autocrine secretion of TGF-β2 by targeting ZNF217 via miR-200c in keloid fibroblasts. Sci Rep 6: 24728, 2016.
8. Liang X, Ma L, Longxand Wang X: lncRNA expression profiles and validation in keloid and normal skin tissue. Int J Oncol 47: 1829-1838, 2015.
9. Schult D, Hölsken A, Siegel S, Buchfelder M, Fahlbusch R, Kreitschmann-Andermahr I and Buslei R: EZH2 is highly expressed in pituitary adenomas and associated with proliferation. Sci Rep 5: 16965, 2015.
10. Liu F, Gu L, Cao Y, Fan X, Zhang F and Sang M: Aberrant over-expression of EZH2 and H3K27me3 serves as poor prognostic biomarker for esophageal squamous cell carcinoma patients. Biomarkers 50: 1-11, 2015.
11. Bae WK, Yoo KH, Lee JS, Kim Y, Chung IJ, Park MH, Yoon JH, Furth PA and Hennighausen L: The methyltransferase EZH2 is not required for mammary cancer development, although high EZH2 and low H3K27me3 correlate with poor prognosis of ER-positive breast cancers. Mol Carcinog 54: 1172-1180, 2015.
12. Li CP, Cai MY, Jiang LJ, Mai SJ, Chen JW, Wang FW, Liao YJ, Chen WH, Jin XH, Pei XQ, *et al*: CLDN14 is epigenetically silenced by EZH2-mediated H3K27ME3 and is a novel prognostic biomarker in hepatocellular carcinoma. Carcinogenesis 37: 557-566, 2016.
13. Appelmann I, Scuoppo C, Thapar V, Ledezma D, Lujambio A, Lowe SW and Chicas A: Suppression of EZH2 accelerates MYC-driven lymphomagenesis by inhibition of apoptosis. Blood 124: 3009, 2014.
14. Xie L, Zhang Z, Tan Z, He R, Zeng X, Xie Y, Li S, Tang G, Tang H and He X: MicroRNA-124 inhibits proliferation and induces apoptosis by directly repressing EZH2 in gastric cancer. Mol Cell Biochem 392: 153-159, 2014.
15. Zhu L and Xu PC: Downregulated lncRNA-ANCR promotes osteoblast differentiation by targeting EZH2 and regulating Runx2 expression. Biochem Biophys Res Commun 432: 612-617, 2013.
16. Luo M, Li Z, Wang W, Zeng Y, Liu Z and Qiu J: Long non-coding RNA H19 increases bladder cancer metastasis by associating with EZH2 and inhibiting E-cadherin expression. Cancer Lett 333: 213-221, 2013.
17. Trenkmann M, Brock M, Bertoncelj MF, Gay RE, Michel BA, Huber LC and Gay S: THU0115 epigenetic repression of the long noncoding Rna hotair regulates NF-κB signalling and the expression of matrix metalloproteases in synovial fibroblasts. Ann Rheum Dis 72: (Suppl 3), 2013.
18. Sarmento O1, Xiong Y, Sun Z, Svingen P, Bamidele A, Smyrk T, Nair A, Baheti S, McGovern D, Friton J, *et al*: O-015 YI Alterations in the FOXP3-EZH2 pathway associates with increased susceptibility to colitis in both mice and human. Inflamm Bowel Dis 22 (Suppl 1): S5-S6, 2016.
19. Varambally S, Cao Q, Mani RS, Shankar S, Wang X, Ateeq B, Laxman B, Cao X, Jing X, Ramnarayanan K, *et al*: Genomic loss of microRNA-101 leads to overexpression of histone methyltransferase EZH2 in cancer. Science 322: 1695-1699, 2008.
20. Coe BP, Thu KL, Aviel-Ronen S, Vucic EA, Gazdar AF, Lam S, Tsao MS and Lam WL: Genomic deregulation of the E2F/Rb pathway leads to activation of the oncogene EZH2 in small cell lung cancer. PLoS One 8: e71670, 2013.
21. Zhou B, Jing XY, Wu JQ, Xi HF and Lu GJ: Down-regulation of long non-coding RNA LET is associated with poor prognosis in gastric cancer. Int J Clin Exp Pathol 7: 8893-8898, 2014.
22. Kalantar Motamedi MH, Heydari M, Heydari M and Ebrahimi A: Prevalence and pattern of facial burns: A 5-year assessment of 808 patients. J Oral Maxillofac Surg 73: 676-682, 2015.
23. Cassidy JT, Phillips M, Fatovich D, Duke J, Edgar D and Wood F: Developing a burn injury severity score (BISS): Adding age and total body surface area burned to the injury severity score (ISS) improves mortality concordance. Burns 40: 805-813, 2014.
24. Jiang T, Wang X, Wu W, Zhang F and Wu S: Let-7c miRNA Inhibits the proliferation and migration of heat-denatured dermal fibroblasts through down-regulating HSP70. Mol Cells 39: 345-351, 2016.
25. Boncler M, Różalski M, Krajewska U, Podsędek A and Watala C: Comparison of PrestoBlue and MTT assays of cellular viability in the assessment of anti-proliferative effects of plant extracts on human endothelial cells. J Pharmacol Toxicol Methods 69: 9-16, 2014.
26. Jiao P, Zhou YS, Yang JX, Zhao YL, Liu QQ, Yuan C and Wang FZ: MK-2206 induces cell cycle arrest and apoptosis in HepG2 cells and sensitizes TRAIL-mediated cell death. Mol Cell Biochem 382: 217-224, 2013.
27. Livak KJ and Schmittgen TD: Analysis of relative gene expression data using real- time quantitative PCR and the 2(-Delta Delta C(T)) Method. Methods 25: 402-408, 2001.

28. Yang KY and Chen DL: Shikonin inhibits inflammatory response in rheumatoid arthritis synovial fibroblasts via lncRNA-NR024118. Evid Based Complement Alternat Med 2015: 631737, 2015.
29. Chinaranagari S, Sharma P and Chaudhary J: EZH2 dependent H3K27me3 is involved in epigenetic silencing of ID4 in prostate cancer. Oncotarget 5: 7172-7182, 2014.
30. Au SL, Wong CC, Lee JM, Wong CM and Ng IO: EZH2-Mediated H3K27me3 is involved in epigenetic repression of deleted in liver cancer 1 in human cancers. PLoS One 8: e68226-e68226, 2013.
31. Qi W, Chan H, Teng L, Li L, Chuai S, Zhang R, Zeng J, Li M, Fan H, Lin Y, *et al*: Selective inhibition of Ezh2 by a small molecule inhibitor blocks tumor cells proliferation. Proc Natl Acad Sci USA 109: 21360-21365, 2012.
32. DuPage M, Chopra G, Quiros J, Rosenthal WL, Morar MM, Holohan D, Zhang R, Turka L, Marson A and Bluestone JA: The chromatin-modifying enzyme Ezh2 is critical for the maintenance of regulatory T cell identity after activation. Immunity 42: 227-238, 2015.
33. Hui T, A P, Zhao Y, Wang C, Gao B, Zhang P, Wang J, Zhou X and Ye L: EZH2, a potential regulator of dental pulp inflammation and regeneration. J Endod 40: 1132-1138, 2014.
34. Dreger H, Ludwig A, Weller A, Baumann G, Stangl V and Stangl K: Epigenetic suppression of iNOS expression in human endothelial cells: A potential role of Ezh2-mediated H3K27me3. Genomics 107: 145-149, 2016.
35. Liu G, Wang T, Wang T, Song J and Zhou Z: Effects of apoptosis-related proteins caspase-3, Bax and Bcl-2 on cerebral ischemia rats. Biomed Rep 1: 861-867, 2013.
36. Liang K, Ye Y, Wang Y, Zhang J and Li C: Formononetin mediates neuroprotection against cerebral ischemia/reperfusion in rats via downregulation of the Bax/Bcl-2 ratio and upregulation PI3K/Akt signaling pathway. J Neurol Sci 344: 100-104, 2014.
37. Wang Q, Liu S, Tang Y, Liu Q and Yao Y: MPT64 protein from *Mycobacterium tuberculosis* inhibits apoptosis of macrophages through NF-kB-miRNA21-Bcl-2 pathway. PLoS One 9: e100949-e100949, 2014.
38. Xu M, Chen X, Han Y, Ma C, Ma L and Li S: Clusterin silencing sensitizes pancreatic cancer MIA-PaCa-2 cells to gmcitabine via regulation of NF-kB/Bcl-2 signaling. Int J Clin Exp Med 8: 12476-12486, 2015.
39. Yap JL, Cao X, Vanommeslaeghe K, Jung K-Y, Peddaboina C, Wilder PT, Nan A, MacKerell AD Jr, Smythe WR and Fletcher S: Relaxation of the rigid backbone of an oligoamide-foldamer-based α-helix mimetic: Identification of potent Bcl-xL inhibitors. Org Biomol Chem 10: 2928-2933, 2012.
40. Yue J, Ben Messaoud N and López JM: Hyperosmotic shock engages two positive feedback loops through caspase-3-dependent proteolysis of JNK1-2 and Bid. J Biol Chem 290: 30375-30389, 2015.
41. Abraham RT, Vanarsdale T, Shields DV, Lee NV, Koehler M and Arndt K: Abstract SY34-03: Braking the cycle: Inhibition of the cyclin D-Cdk4/6 pathway in breast cancer. Cancer Res 74 (19 Supplement): 772-779, 2014.
42. Rader J, Russell MR, Hart LS, Nakazawa MS, Belcastro LT, Martinez D, Li Y, Carpenter EL, Attiyeh EF, Diskin SJ, *et al*: Dual CDK4/CDK6 inhibition induces cell-cycle arrest and senescence in neuroblastoma. Clin Cancer Res 19: 6173-6182, 2013.
43. Pils D, Bachmayr-Heyda A, Auer K, Svoboda M, Auner V, Hager G, Obermayr E, Reiner A, Reinthaller A, Speiser P, *et al*: Cyclin E1 (CCNE1) as independent positive prognostic factor in advanced stage serous ovarian cancer patients - a study of the OVCAD consortium. Eur J Cancer 50: 99-110, 2014.